Pergamon

Cement and Concrete Research, Vol. 28, No. 5, pp. 727–736, 1998

0008-8846/98 $19.00 + .00

PII S0008-8846(98)00035-0

EFFECT OF THE TRANSITION ZONE ON THE ELASTIC MODULI OF MORTAR

C.C. Yang
Institute of Materials Engineering, National Taiwan Ocean University, Keelung, Taiwan, Republic of China

(Received December 6, 1996; in final form March 9, 1998)

ABSTRACT

In order to investigate the behavior of transition zone and the effect of transition zone on the elastic modulus of mortar, cubic specimens (50 × 50 × 50 mm) with different volume fractions (volume of aggregate/volume of mortar, a/t = 0.0, 0.1, 0.2, 0.3, 0.4, and 0.5) of aggregate were cast and tested. The Double-Inclusion method and Mori-Tanaka theory were used to predict the elastic moduli of three-phase (aggregate, transition zone, and cement paste) composite materials. A comparison was also made between the theoretical results and experimental data. Based on this comparison, when the thickness of transition zone is 20 μm, the average Young's modulus of transition zone is about 20 to 40% of the matrix modulus. When the thickness of transition zone is 40 μm, the average Young's modulus of transition zone is about 50 to 70% of the matrix modulus. Test results show that the overall elastic properties of the composite depend mainly on the volume fraction of aggregate. *© 1998 Elsevier Science Ltd*

Introduction

In concrete, the hydrated mortar surrounding the aggregate has different microstructures resulting from the water/cement ratio gradient developed at the interfacial layer (1). This layer around the aggregate is called the transition zone. Many researchers have measured the microstructure of transition zone in cement-based materials by use of scanning electron microscopy (SEM) (2–6), energy-dispersion X-ray spectrometry (EDX) (7–8), and back-scattered electron (BSE) imaging (9–10). The porosity of the transition zone was applied to measure the mercury intrusion porosimetry (MIP) (11–12). Li et al. (13–14) characterized the interfacial properties using pullout tests. Alexander (15) used two experimental techniques to estimate the interfacial properties of cement-based composite.

As pointed out by Monteiro (16) the influence of the transition zone has already been established for the compressive strength of concrete. However, little work has been done in assessing transition zone effect on the elastic moduli of concrete. By considering concrete as a two-phase material, Aïtcin and Mehta (1)and Baalbaki et al. (17) demonstrated that the elastic modulus of concrete was influenced by the elastic properties and volume fraction of aggregates. Stock et al. (18) also obtained the elastic moduli of mortar and concrete with different aggregate volume fractions by experiment. Hirsch (19) derived a semi-empirical equation for the elastic modulus of concrete. For composite mechanics, Voigt's (20) approximation yielded the parallel model and the Reuss's (21) approximation yielded the series model of the average elastic moduli. Monteiro (16) pointed out that parallel and series models were obtained without consideration of the interface geometry or the "degree of bond." Hashin and Shtrikman (22) proposed the variational principle to find the Hashin-Shtrikman (H-S) bounds on the average elastic moduli of composite materials. Monteiro (16) suggested that H-S bounds can be used to asses the effect of transition zone on elastic moduli of cement-based materials. Nilsen and Monteiro (23) evaluated H-S bounds using Hirsh's data (19) and found that transition zone has a significant effect on the overall elastic moduli of mortars. Lutz and Monteiro (24) modeled the interfacial effect of transition zone by assuming that the elastic moduli vary in the vicinity of the inclusions following a power law. Cohen et al. (25) proposed that the dynamic elastic moduli of cement paste and silica fume mortars are a function of surface area and of hydration time. Ramesh et al. (26) have investigated the effect of the elastic modulus and volume fraction of the transition zone on the overall elastic modulus of cement-based composite and a model for evaluation of the elastic moduli of concrete was derived. Simeonov and Ahmad (27) have also used H-S bounds to assess the effect of the transition zone on elastic modulus of cement-based composite and pointed out the properties of transition zone are related to the water content of the cement matrix. Using a hard core/soft shell computer model, Winslow et al. (28) investigated the percolation characteristics of the interfacial zone of mortar and concrete. Zimmerman et al. (29) investigated the influence of pores on the elastic moduli of mortar and the experimental results were compared with the Kuster-Tolsöz theory (30).

Mori and Tanaka (31) applied the concept of average field to analyze macroscopic properties of composite materials. The average field in a body contains inclusions with eigenstrain. In addition, the shape effect of dispersoids was introduced in Eshelby's (32) method to assess the properties of composite materials. The development of evaluating overall elastic modulus and overall elastic-plastic behavior of the composites was reviewed by Mura (33). In order to make a better prediction, Hori and Nemat-Nasser (34) suggested a model taking the interface layer into account for a two-phase composite.

In this study, mortar is considered as a composite material in which sand particles are embedded in a matrix of hardened cement paste, and the transition zone is around the sand particles. The elastic moduli of mortars were obtained in the laboratory. Hori and Nemat-Nasser's double inclusion model (34) for a two-phase composite was used to evaluate the equivalent elastic moduli of the aggregate with a transition zone. An approach of average elastic relationships of mortar with the inhomogeneities (aggregate with transition zone) is evaluated in this study by employing the Mori-Tanaka theory (31).

Experimental Program

In this study, the composite was composed of cement paste, fine aggregate, and transition zone. Mortars were made with ordinary Type I cement, silica fume, and Ottawa sand. The fine aggregate passing #30 sieve and retained on #50 sieve was used. The proportions of the mortar are summarized in Table 1; all the mixtures had a water/binder ratio of 0.30, and the superplasticizer was adjusted to keep the flow of the paste the same. In order to study the effect of the aggregate and transition zone on the elastic modulus of mortar, six different

TABLE 1
Mix design and volume fraction of aggregate.

design -ation	water (Kg/m^3)	cement (Kg/m^3)	sand (Kg/m^3)	silica fume (Kg/m^3)	SP (Kg/m^3)	*volume fraction (%)
M0	442.1	1426.2	0	142.6	28.5	0
M1	397.2	1281.4	261.8	128.1	25.6	10
M2	352.4	1136.6	523.6	113.7	22.7	20
M3	307.5	991.8	785.4	99.2	19.8	30
M4	262.6	847.0	1047.2	84.7	16.9	40
M5	217.7	702.3	1309.0	70.2	14.1	50

*(the volume of sand)/(the volume of mortar).

volume fractions f_a(a/t = 0.0, 0.1, 0.2, 0.3, 0.4, and 0.5) of fine aggregate were selected in the mix proportions. The densities of the constituent materials are listed in Table 2.

The cubic specimens (50 × 50 × 50 mm) were cast and cured in the laboratory. For determining the elastic moduli of the mortars, two axial electric strain gages (gage length = 10 mm) were mounted on opposing sides of specimen to measure the compressive strains. The compressive test was conducted using a 100-ton universal testing machine according to the specification of ASTM C87. The load was applied at a constant rate within the range of 0.14 ~ 0.34 MPa/s. Continuous measurements were recorded to obtain the stress/strain curves and the secant modulus was determined from the stress/strain curves.

Results and Discussions

By considering cement-based materials as a three-phase (cement paste, fine aggregate, and transition zone) composite material, the spherical shape of fine aggregate is modeled and the transition zone is considered as a uniform layer around the aggregate. The aggregate with associated transition zone and matrix is considered as a heterogeneous inclusion. In this study, inclusions are randomly embedded in an infinite matrix and the inclusions with transition zone are not overlapped (see Fig. 1). The calculation is divided into two stages. In the first stage, the equivalent elastic moduli of aggregate and transition zone were calculated by Hori and Nemat-Nasser's double inclusion model (34). In the second, the Mori-Tanaka theory (31) was used to calculate the overall elastic moduli of the composite.

TABLE 2
Densities of the constituent materials (g/cm^3).

water	cement	sand	silica fume	SP
1.0	3.15	2.618	2.150	1.2

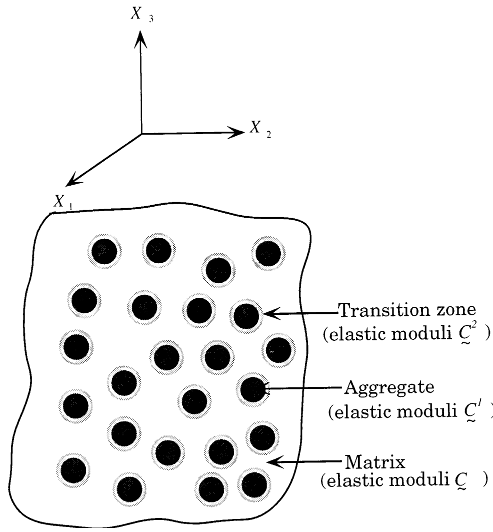

FIG. 1.

Aggregates are modeled as spherical shape and transition zone as a layer around the aggregates which embedded in matrix.

Double-Inclusion Method

The double-inclusion method (34) is applied to calculate the equivalent elastic modulus of aggregate and transition zone. A sufficiently large body *B* is assumed to contain two types of inclusions. Aggregate is one inclusion, having elastic moduli $\underset{\sim}{C}^1$; transition zone, with elastic moduli $\underset{\sim}{C}^2$, is considered as the other inclusion. The domain surrounding the inhomogeneities is referred to as the matrix (cement paste) *B*, which has elastic moduli $\underset{\sim}{C}$ (Fig. 2). When *R* and Ω are similar and coaxial spheres, the equivalent average elastic moduli of the aggregate and transition zone, $\underset{\sim}{C}^{E}$, is given as (34):

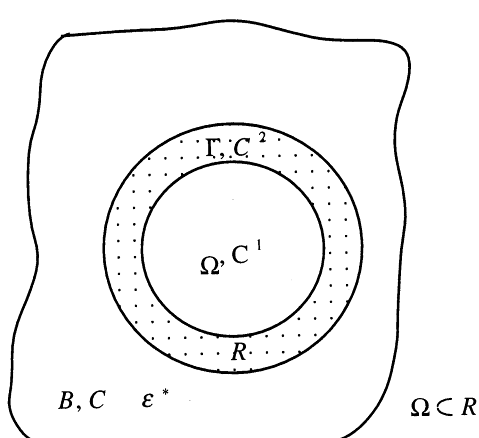

FIG. 2.
Double-inclusion model (after Hori and Nemat-Nasser (34)).

TABLE 3
The equivalent elastic moduli of the aggregate and transition zone (GPa).

cement paste E_m	sand E_m	h = 20 μm, (V_f = 0.7745) transition zone (TZ) E_t		h = 20 μm, (V_f = 0.7745) equivalent of (sand + TZ) E_e	h = 40 μm, (V_f = 0.6121) transition zone (TZ) E_t		h = 40 μm, (V_f = 0.6121) equivalent of (sand + TZ) E_e
		0.6 E_m	12.456	47.854	0.9 E_m	18.684	42.098
		0.5 E_m	10.380	45.768	0.8 E_m	16.608	40.011
20.76	80.	0.4 E_m	8.304	43.535	0.7 E_m	14.532	37.836
		0.3 E_m	6.228	41.140	0.6 E_m	12.456	35.569
		0.2 E_m	4.152	38.563	0.5 E_m	10.380	33.202
		0.1 E_m	2.076	35.783	0.4 E_m	8.304	30.729

$$\underset{\sim}{C}^{E} = [\underset{\sim}{I} + (\underset{\sim}{S} - \underset{\sim}{I})\,\underset{\sim}{A}](\underset{\sim}{I} + \underset{\sim}{S}\,\underset{\sim}{A})^{-1} \tag{1}$$

where $\underset{\sim}{A}$ is defined as

$$\underset{\sim}{A} = \underset{\sim}{V}_f\,(\underset{\sim}{A}^{\Omega} - \underset{\sim}{S})^{-1} + (1 - \underset{\sim}{V}_f)(\underset{\sim}{A}^{R} - \underset{\sim}{S})^{-1}$$

and

$$\underset{\sim}{A}^{\Omega} = (\underset{\sim}{C} - C^{1})^{-1}\,\underset{\sim}{C}$$

$$\underset{\sim}{A}^{R} = (\underset{\sim}{C} - \underset{\sim}{C}^{2})^{-1}\,\underset{\sim}{C}$$

where V_F is the volume fraction of Ω in R and $\underset{\sim}{I}$ is the unit tensor. $\underset{\sim}{S}$ is the Eshelby tensor for a single inclusion which solely exists in an infinite homogeneous medium. The Eshelby tensor is a function of the geometry of the inclusion and Poisson's ratio of the matrix (see appendix). In this study, the fine aggregate particles are assumed to be spherical.

The transition zone thickness is usually selected as a region between 30 and 50 μm. In this study, the transition zone is assumed to have a width between 20 μm (28) and 40 μm. The average size of fine aggregate particle is 450 μm. When the thickness of transition zone h is 20 μm, the volume fraction of Ω in R ($\Omega = (225\ \mu m)^3$, $R = (245\ \mu m)^3$, see Fig. 1) is 0.7745. When the thickness of transition zone is 40 μm, the volume fraction of Ω in R is 0.6121.

The elastic modulus of cement paste is 20.76 GPa, which was obtained directly from the experiment. The empirical elastic modulus of aggregate (E_a) is 80 GPa and the Poisson ratio of aggregate (v_a) and cement paste (V_m) is 0.21 and 0.2, respectively. Because it is difficult to test the transition zone separately, little information is available for the material properties of the transition zone. In this study, the elastic modulus of transition zone E_t is assumed to be various percentages of cement paste elastic modulus for the purpose of calculating the equivalent elastic moduli of the aggregate and transition zone. The equivalent elastic moduli of the aggregate and transition zone (the R domain in Fig. 2), $\underset{\sim}{C}^{E}$, were obtained from Eq. 1 and the results are listed in Table 3.

TABLE 4
The measured and calculated eleastic moduli of mortars.

designation	f_a (%)	E_c (GPA) *(Measured)	E_c^* (GPA) (Calculated)	$\frac{E_c^* - E_c}{E_c} \times 100$ (%)
M0	0	20.760	—	—
M1	10	22.304	23.354	4.71
M2	20	24.141	26.293	8.91
M3	30	26.350	29.652	12.53
M4	40	29.292	33.527	14.46
M5	50	32.439	38.048	17.29

*Average of three specimens.

Overall Elastic Moduli of Cement-Based Materials

In the previous work (35), the overall average elastic moduli of cement-based composite $\bar{\underset{\sim}{C}}$ was given by

$$\underset{\sim}{C} = \{\underset{\sim}{C}^{-1} + f[\{(1-f)(\underset{\sim}{C}^{E} - \underset{\sim}{C})\underset{\sim}{S} - f(\underset{\sim}{C} - \underset{\sim}{C}^{E}) + \underset{\sim}{C}\}^{-1}](\underset{\sim}{C} - \underset{\sim}{C}^{E})\underset{\sim}{C}^{-1}\}^{-1} \qquad (2)$$

where the volume fraction of aggregate with transition zone is expressed as f.

For computing the overall elastic moduli of three-phase cement-based materials, the equivalent elastic moduli of the aggregate and transition zone (see Table 2) were used. The Poisson's ratio of the aggregate and transition zone is considered the same as the cement paste. Three different thicknesses of transition zone (h = 0 μm, 20 μm, and 40 μm) were considered, respectively.

h = *0 μm (two-phase composite).* In this case, the elastic moduli of transition zone is equal to the cement paste, and the cement-based material is a two-phase composite material. The elastic moduli of mortars were obtained using Eq. 2. The measured and calculated elastic moduli of mortars are presented in Table 4.

Figure 3 illustrates the relationship between volume fraction of aggregate $f_a$and elastic modulus of two-phase composite (mortar). The experimental results with the calculated results are also shown in Figure 3. It can be seen from the figure that the mortar elastic modulus increases with an increase in aggregate volume fraction. Test data were below the theoretical results obtained from a two-phase model. It was found that the overall elastic modulus of cement-based composite was affected by the transition zone (23,36). Therefore, it is reasonable to consider the third phase (transition zone) in the analytical prediction.

h = *20 μm (three-phase composite).* For computing the overall elastic moduli of three-phase cement-based materials with a transition zone thickness of 20 μm (h = 20 μm), the equivalent elastic moduli of the aggregate and transition zone were calculated from Eq. 1 (see Table 3). The elastic modulus and Poisson's ratio of cement paste were obtained following previous procedure. The overall elastic modulus of three-phase cement-based materials is calculated from Eq. 2. Figure 4 shows the relationship between mortar elastic modulus and the aggregate volume fraction. The corresponding theoretical results are also illustrated in the

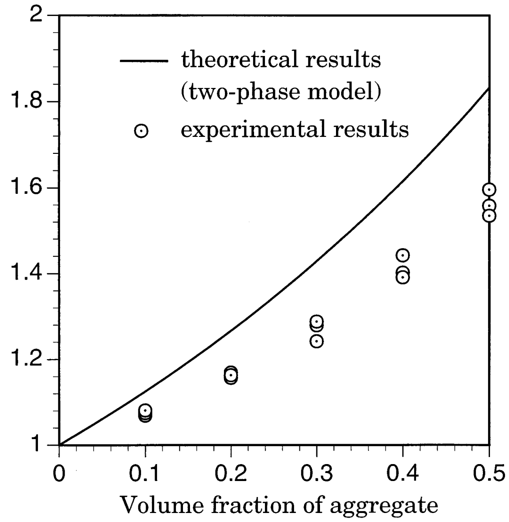

FIG. 3.
Volume fraction of aggregate vs. E_c/E_m curves ($h = 0$ μm).

figure. The graph correlates the volume fraction of the aggregate with the elastic modulus of the composite for different interface properties. By comparing the experimental data with the theoretical results, it can be seen that the higher aggregate volume fraction, the difference of E_c/E_m considering various e_t, is more significant than for the lower aggregate volume fractions. It appears that the third phase (transition zone) becomes more significant as the volume fraction of aggregate increases. The test results are within the curves of $E_t = 0.2\ E_m$ and $E_t = 0.4\ E_m$. It shows that the transition zone effect is significant in the composite.

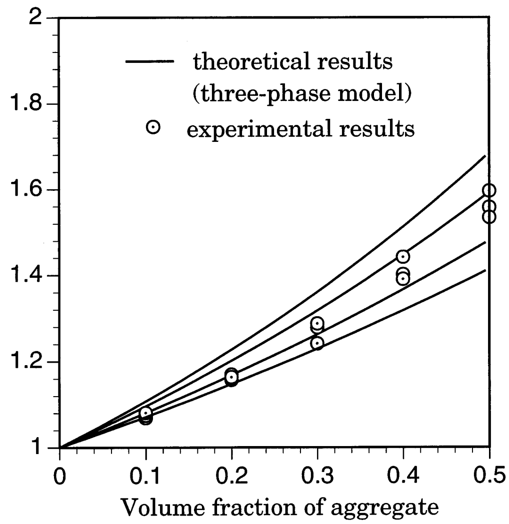

FIG. 4.
Volume fraction of aggregate vs. E_c/E_m curves.

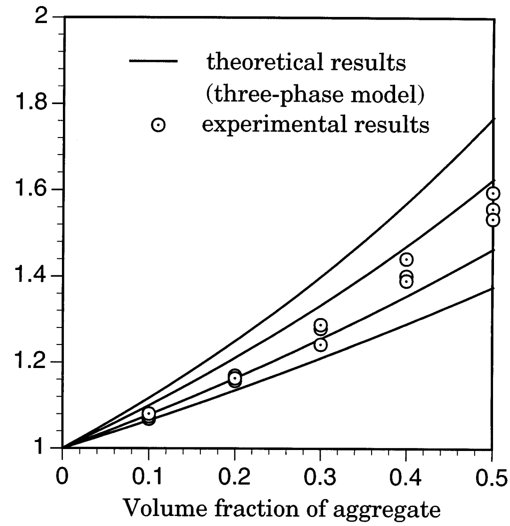

FIG. 5.
Volume fraction of aggregate vs. E_c/E_m curves.

h = *40 μm (three-phase composite).* In this case, a 40-μm thick interface zone was assumed to surround the sand particle. The equivalent elastic moduli of the aggregate and transition zone are shown in Table 3. The previous elastic properties were used. Figure 5 shows the relationship between mortar elastic moduli and the aggregate volume fraction. The corresponding theoretical results are also illustrated in the figure. The graph correlates the volume fraction of the aggregate with the elastic modulus of the composite for various properties of transition zone. By taking the 40-μm thick interface zone, test results are within the curves of $E_t = 0.5\ E_m$ and $E_t = 0.7\ E_m$.

Conclusions

The elastic modulus of mortar is influenced by the elastic properties and volume fraction of the aggregate and transition zone. The elastic modulus of mortar increases with an increase in volume fraction of fine aggregate. The volume of transition zone depends on the total aggregate surface area and the interface thickness. Based on the analytical and experimental results, the average elastic modulus of transition zone is about 20 to 40% of the matrix modulus for the transition zone with a thickness of 20 μm, and the average elastic modulus of transition zone is about 50 to 70% of the matrix modulus for the transition zone with a thickness of 40 μm.

The Double-Inclusion method and the Mori-Tanaka theory is suitable for estimating the elastic moduli of mortar by taking three phases into account (cement paste, aggregate, and transition zone). This study initiates the evaluation of the transition zone effect using micromechanics. More extensive and more refined researches need to be done to ascertain the properties and thickness of transition zone.

Acknowledgment

The support of NSC Contract No. NSC 86–2221 - E - 019–002 is gratefully appreciated.

References

1. P.C. Aïtcin and P.K. Mehta, ACI Mat. J. 87, 103 (1990).
2. S. Diamond and S. Mindess, Cem. Concr. Res. 22, 67 (1992).
3. S. Diamond and S. Mindess, Cem. Concr. Res. 22, 678 (1992).
4. S. Diamond and S. Mindess, Cem. Concr. Res. 24, 1140 (1994).
5. K.L. Scrivener, A. Bentur, and P.L. Pratt, Adv. Cem. Res. 1, 230 (1988).
6. K. L. Scrivener and A. Bentur, Proceedings of the 8th Intl. Congress of the Chemistry of Cement, III, 466 (1986).
7. T. Sugama, N. Carciello, L. E. Kukacka, and G. Gray, J. Mater. Sci. 27, 2863 (1992).
8. Y. Wang, S. Li, Y. Lu, and M. Su, Proceedings of the 9th Intl. Congress on the Chemistry of Cement, V, 184 (1992).
9. P. Raivio and L. Sarvaranta, Cem. Concr. Res. 24, 896 (1994).
10. K.L. Scrivener and K.M. Nemati, Cem. Concr. Res. 26, 35 (1996).
11. M. Hoshino, Mater. Struc. 21, 336 (1988).
12. A. Goldman and A. Bentur, Interfaces in Cementitious Composites, RILEM Intl. Conf., 53 (1992).
13. Z. Li, B. Mobasher, and S.P. Shah, J. Am. Ceram. Sci. 74, 2156 (1991).
14. Z. Li, S.P. Shah, and M.J. Aquino, Microstructure of Cement-Based Systems/Bonding and Interfaces in Cementitious Materials, MRS Proceedings, 370, 319 (1994).
15. M.G. Alexander, Cem. Concr. Res. 23, 567 (1993).
16. P.J. Monteiro, Cem. Concr. Res. 21, 947 (1991).
17. W. Baalbaki, B. Benmokrane, O. Chaallal, and P.C. Aïtcin, ACI Mat. J. 88, 499 (1991).
18. A.F. Stock, D.J. Hannant, and R.I.T. Wiliams, Mag. Concr. Res. 31, 225 (1979).
19. T.J. Hirsch, J. ACI 427 (1962).
20. W. Voigt, Wied. Ann. 38, 573 (1889).
21. A. Reuss, Z. Angew. Math. Mech. 9, 49 (1929).
22. Z. Hashin and S. Shtrikman, J. Mech. Phys. Solids 10, 335 (1962).
23. A.U. Nilsen and P.J.M. Monteiro, Cem. Concr. Res. 23, 147 (1993).
24. M.P. Lutz and P.J.M. Monteiro, Microstructure of Cement-Based Systems/Bonding and Interfaces in Cementitious Materials, MRS Proceedings, 370, 413 (1995).
25. M.D. Cohen, A. Goldman, and W.F. Chen, Cem. Concr. Res. 24, 95 (1994).
26. G. Ramesh, E.D. Sotelino, and W.F. Chen, Cem. Concr. Res. 26, 611 (1996).
27. P. Simeonov and S. Ahmad, Cem. Concr. Res. 25, 165 (1995).
28. D.N. Winslow, M.D. Cohen, D.P. Bentz, K.A. Snyder, and E.J. Garboczi, Cem. Concr. Res. 24, 25 (1994).
29. R.W. Zimmerman, M.S. King, and P.J.M. Monteiro, Cem. Concr. Res. 16, 239 (1986).
30. G.T. Kuster and M.N. ToksÖz, Geophysics 39, 587 (1974).
31. T. Mori and K. Tanaka, Acta Metall. 21, 571 (1973).
32. J. D. Eshelby, Proc. Roy. Soc. A241, 376 (1957).
33. T. Mura, Applied Mech. Reviews 41, 15 (1988).
34. S. Nemat-Nasser and M. Hori, Micromechanics: Overall Properties of Heterogeneous Materials, North-Holland, 1993.
35. C.C. Yang, R. Huang, W.D. Yeih, and J.J. Chang, The Chinese J. of Mech. 11, 47 (1995).
36. J.C. Maso (ed.), Interfacial Transition Zone in Concrete, RILEM report 11, E & FN SPON, 1996.
37. T. Mura, Micromechanics of Defects in Solids, Second Revised Edition, Martinus Nijhoff Publishers, 1987.

Appendix

The Eshelby's tensor $\underset{\sim}{S}$ for sphere inclusion is listed below (37).

$$S_{1111} = \frac{7-5v}{15(1-v)}, \qquad S_{2222} = \frac{7-5v}{15(1-v)}, \qquad S_{3333} = \frac{7-5v}{15(1-v)}.$$

$$S_{1122} = \frac{5v-1}{15(1-v)}, \qquad S_{2233} = \frac{5v-1}{15(1-v)}, \qquad S_{3311} = \frac{5v-1}{15(1-v)}.$$

$$S_{1133} = \frac{5v-1}{15(1-v)}, \qquad S_{2211} = \frac{5v-1}{15(1-v)}, \qquad S_{3322} = \frac{5v-1}{15(1-v)}.$$

$$S_{1212} = \frac{4-5v}{15(1-v)}, \qquad S_{2323} = \frac{4-5v}{15(1-v)}, \qquad S_{3131} = \frac{4-5v}{15(1-v)}.$$